Hindawi
Journal of Nanomaterials
Volume 2020, Article ID 5239474, 9 pages
https://doi.org/10.1155/2020/5239474

Research Article

Preparation of Sol-Enhanced Ni–P–Al_2O_3 Nanocomposite Coating by Electrodeposition

Yongfeng Li,[1] **Kun Zhang**,[1] **Mingming Zhang**,[1] **Yaqi Zhang**,[1] **Tingting Wu**,[1] **Hongyuan Zhao**,[1] **Jianxiu Su**,[1] **Zhankui Wang**,[1] **and Junfeng Wang**[2]

[1]*School of Mechanical and Electrical Engineering, Henan Institute of Science and Technology, East of Hualan Road, Xinxiang 453003, China*
[2]*Xinxiang Yuke Mechanical and Electrical Equipment Co., Ltd, Wangcun Town, Muye District, Xinxiang 453003, China*

Correspondence should be addressed to Yongfeng Li; lyf16816800@163.com

Received 7 January 2020; Revised 25 March 2020; Accepted 7 April 2020; Published 18 May 2020

Academic Editor: David Cornu

A Ni–P–(sol)Al_2O_3 coating was prepared on the surface of Q235 steel by direct-current electrodeposition. This method was combined with sol-gel and electrodeposition technique, instead of the traditional nanopowder dispersion, to prepare highly dispersible oxide nanoparticle-reinforced composites. The effects of temperature, pH value, and current density and Al_2O_3 sol on the hardness of composite coating were investigated. The coating surface morphology and structure were characterized by scanning electron microscopy and energy dispersive spectroscopy, respectively. The corrosion resistance of coatings in the presence of intermediate layers was evaluated by electrochemical measurement in 3.5% NaCl solution by open-circuit potential measurement at room temperature. The hardness and wear resistance of the coating were measured by a microindentation instrument and friction wear machine, respectively. The results showed that Al_2O_3 sol can effectively improve Ni–P alloy coating structure and refine grain. When the bath temperature was 55°C, the pH value was 4.5, the amount of sol was 80 mL/L, the current density was 1 A/dm^2, and the hardness of the nanosol coating was 569 HV. Compared with Ni–P, the friction coefficient increases slightly, but the wear rate was only 1.768×10^{-6} g · m^{-1}. The corrosion resistance was also better than that of Ni–P coating.

1. Introduction

It is a challenge for traditional nickel coating, with the rapid development of modern industry, to meet the special requirements in some harsh conditions. In recent years, how to improve the comprehensive performance of coatings has become a hotspot [1]. Direct current electrodeposition refers to the electrochemical deposition process of metals or alloys from their compound aqueous solution, nonaqueous solution or molten salt. It is the basis of the process of metal electrolytic smelting, electrolytic refining, electroplating, and electroforming. These processes are carried out under certain electrolytes and operating conditions. The difficulty of metal electrodeposition and the shape of the deposit are related to the properties of the deposited metal and also depend on the composition of the electrolyte, pH value, temperature, current density, and other factors. Ni-based alloys show several attractive properties, such as its high hardness [2], toughness, and relatively good corrosion resistance in air. For these reasons, they become the first choice of protective coating materials. However, the phosphorous nickel alloy coating obtained by electroless Ni–P plating is prone to pinholes and other defects on the surface, and the porosity and morphology will directly affect the corrosion resistance of the nickel-phosphorus alloy coating [3]. The corrosion resistance of the coating decreases regardless of whether the penetrating pore is formed or not. Therefore, the researchers tried to add an appropriate amount of inert particles to the plating solution and deposit them with Ni–P to get more excellent composite coating [4]. At present, nano-SiC [5], TiO_2 [6–8], WC [9], SiO_2 [10, 11], PTFE [12, 13], ZrO_2 [14], and Al_2O_3 [15] are common solid particles that can be added. As a widely used ceramic material, alumina is not only of high hardness but also easy to be combined with matrix

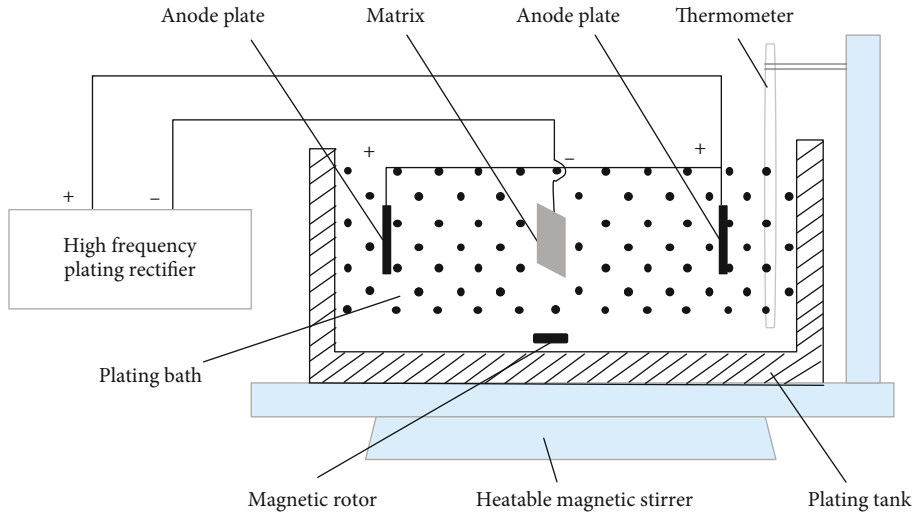

Figure 1: Experimental setup of electrodeposition of Ni–P–(sol)Al_2O_3 nanocomposite coating.

[16–19]. Nanocomposite coating has higher hardness, abrasion resistance, friction reduction, and corrosion resistance than ordinary electroplating. Balarju et al. [20] found that nanoparticles had no effect on the chemical structure of the composite coatings obtained by adding nanoalumina and significantly improved the hardness, corrosion resistance, and wear resistance. However, the so-called composite coatings are prone to some problems. Because nanoparticles have a high energy surface and activity, these nanoparticles are unstable and easily agglomerated in the nickel plating bath without special surface modification. It is difficult to provide enough time for nanoparticles to deposit on the surface of the substrate even if they are stirred at high speed and for a long time. Appropriate dispersants and stabilizers must be added. This issue directly affects homogeneous quality and weakens the mechanical properties of coatings. Alumina sol can effectively avoid the agglomeration of nanoparticles in the coating matrix [21–23] and is rapidly and uniformly dispersed in the plating solution, which is easy to be doped, and the required external conditions are easy to be realized. Alumina sol used in this project, the preparation, and properties of Ni–P–(sol)Al_2O_3 composite coatings were studied.

2. Materials and Methods

2.1. Preparation of Nanocomposite Sol Coating. The substrate specimen used in the experiment was a Q235 cold-rolled steel sheet with a size of $40 \times 25 \times 2\,mm^3$. The substrate was polished with 400, 800, and 1000 grade SiC paper and then washed and rinsed with distilled water.

Figure 1 shows the experimental setup of the electrodeposition of Ni–P–(sol)Al_2O_3 nanocomposite coating. The applied current is provided by a high-frequency plating rectifier. The CS2350 electrochemical workstation is used to provide DC stabilized power supply. The HJ-5 constant temperature magnetic stirrer is used to control the bath temperature and magnetic stirring to ensure uniform solution and dispersion of nanoparticles. The plated part is placed in the middle of the two anode plates to achieve double-sided growth of the plating on the substrate. In addition, it is necessary to ensure that the two anode plates are parallel to the cathode substrate and the distance is kept at 25 mm to ensure the same plating quality on both sides of the plated part.

Table 1: Components of alkali cleaning solution and technological condition.

Composition	Quantity	Drugs and parameters	Quantity
NaOH	35(g/L)	OP-10	2 (g/L)
Na_2CO_3	25 (g/L)	Temperature	85 ± 2 (°C)
Na_3PO_4	10 (g/L)	Time	10-20 (min)
Na_2SiO_3	10 (g/L)		

Workpieces are inevitably contaminated with oil during processing, storage, and transportation. The oil removal formula used in the experiment is shown in Table 1. Then, it is cleaned with deionized water and ultrasonic cleaning is carried out for 2 min.

Pickling is the process of removing oxide film, oxide scale, and rust on the metal surface after oil removal. Hydrochloric acid has strong solubility to metal oxides, slow dissolution to iron and steel matrix, clean surface after pickling, but its acid fog is big, which corrodes equipment. Sulphuric acid also has less corrosion to the matrix and less acid mist, but is prone to overcorrosion and hydrogen embrittlement. In this experiment, the mixture of 15 wt% nitric acid and 5 wt% phosphoric acid was used as a pickling solution.

The purpose of activation is to remove the very thin oxide layer on the surface of the matrix after pickling and to expose the matrix metal evenly so that the coating can grow uniformly on its surface. In this experiment, 5 wt% hydrochloric acid was used for activation. The activation time was 3 min, and the temperature was about 25°C at room temperature. After activation, ultrasonic cleaning was added for 1 minute, and then plating was carried out.

Table 2: Compositions of bath solution.

Bath compositions	Concentration ($g \cdot L^{-1}$)	Depositing parameters	Values
$NiSO_4 \bullet 6H_2O$	230	Temperature (°C)	45, 50, 55, 60
H_3BO_3	30	pH	3.5, 4, 4.5, 5
$NaH_2PO_2 \bullet H2O$	15	Current density (A/dm^2)	0.5, 1, 1.5, 2
$NiCl_2 \bullet 6H_2O$	15	Time (min)	10
Al_2O_3 sol wt20% (60-70 nm)	80 ml/L		
$C_{12}H_{25}SO_4Na$	0.4		

Composition and parameters of composite plating bath as shown in Table 2. Alumina sol is provided by the supplier of crystal Fire Technology Glass Co., Ltd. (http://www.jinghuoglass.cn). The alumina sol specifications were the alumina sol concentration was 20% and the average particle size was 60–70 nm. In order to ensure the quality of the coating, the distance between the two anodic pure nickel plates and the cathode substrate is 25 mm. Prior to the addition of this sol suspension into the bath, Ni–P coating was performed for ten minutes for better adhesion of coatings with the substrate. A reference specimen of plain Ni–P coating was also prepared for the comparative study. The plating bath was agitated using a magnetic stirrer at 180 rpm during the plating course.

2.2. Methods. The Vickers microhardness measurements of the coatings were taken using a VMH–002 V microhardness tester at a load of 50 g for 15 s. The corresponding final values were reported as the average of five measurements. Friction and wear tests were carried out using ball-on-disk method by using a tribometer (MS–T3000 Instruments, China) at a normal load of 500 g rotation speed of 300 r/min under reciprocating sliding motion in a dry condition at the temperature 25–30°C and humidity 25% ± 10%. A bearing steel ball having a diameter of 3 mm was used as a counter sliding partner. The polarization curve of the anode was measured at room temperature using a CS2350 electrochemical workstation, and the corrosion resistance of the coating was evaluated by a Tafel curve. The coating was exposed to a scanning range of -2.0–1.0 V at a scanning rate of 1 mV/s in 3.5 wt% NaCl solution. The auxiliary electrode was a platinum electrode, and the reference electrode was a saturated calomel electrode. The surface and cross-section morphology and chemical composition of the coatings were analyzed by Quanta 200 scanning electron microscope (SEM) coupled with energy-dispersive X-ray spectroscope (EDS).

3. Results and Discussion

3.1. Effect of pH Value on Microhardness of Composite Coating. Figure 2 shows the effect of bath pH value on Ni–P–(sol)Al_2O_3 composite coating at current density $1A/dm^2$. The microhardness of sol composite coating first increases and then decreases with the increase of pH value. This is because the pH value has a critical impact on the nickel deposition process and the mechanical properties of the coating. Near the area with high H^+ concentration, the deposition rate

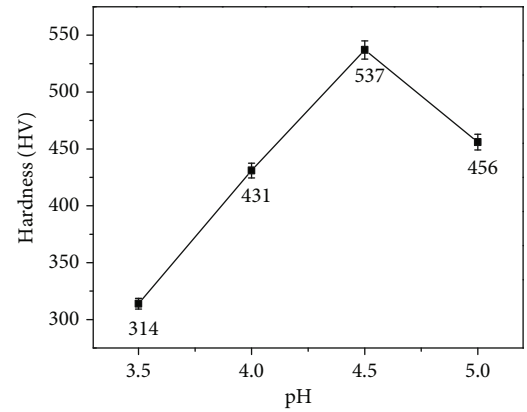

Figure 2: Effect of pH value on microhardness of coating.

is low due to the slow formation and growth of crystal nucleus, resulting in thin coating and no significant improvement in hardness. Similar situations have been reported in a similar pH bath [24, 25]. Besides, it has been pointed out that the pH of the plating solution has an effect on the P content of the coating, that is, the hardness of the coating increases with the decrease of P content [26]. The increase of pH may decrease the P content in the coating. When the pH value of the plating solution reaches 4.5, the microhardness of the sol composite coating was 537 HV at the maximum. As the pH value continues to increase, the coating was mixed with nickel hydroxide and other impurities easily, resulting in rough coating brittle, hardness decline.

3.2. Effect of Temperature on Microhardness of Composite Coating. Figure 3 shows the effect of bath temperature on Ni–P–(sol)Al_2O_3 composite coating at current density $1A/dm^2$ and pH value 4.5. With the increase of temperature, the microhardness of the sol composite coating increases firstly and then decreases. This is explained by an increase in the kinetic driving force with the increase in temperature can lead to a higher nucleation rate, i.e., formation of fine grains. These fine grains effectively inhibited its own growth, and the hardness of the coating increased accordingly [27]. As the temperature continues to increase, the thermodynamic driving force of crystallization decreases with an increase in the critical size of the nucleus resulting to lower nucleus densities, i.e., formation of coarse grain [28, 29]. The formation of such coarse grains is likely to make the structure loose and the hardness of the coating decreased.

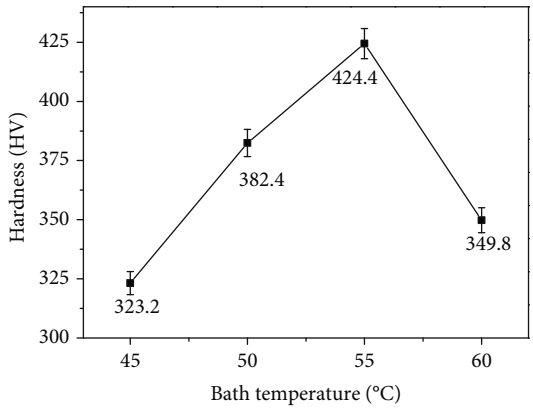

Figure 3: Effect of temperature on microhardness of coating.

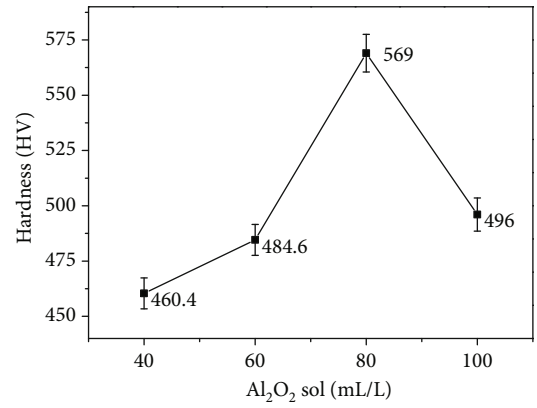

Figure 5: Effect of Al_2O_3 sol on microhardness of coating.

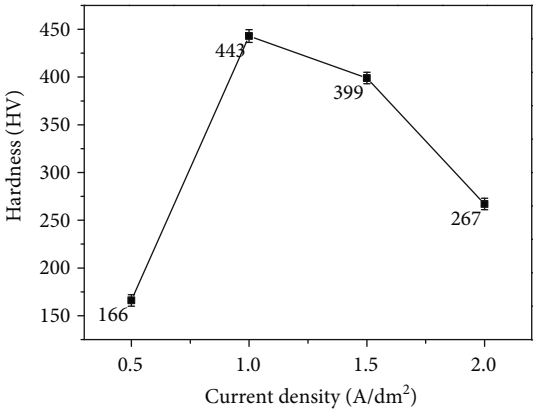

Figure 4: Effect of current density on microhardness of coating.

This discrepancy may occur due to the fact that an increase in the bath temperature has two contradictory effects on the thermodynamic and kinetic driving force [27]. Moreover, as the temperature is too high, the viscosity of the plating solution decreases, the adhesion force of the cathode surface decreases [30, 31], and the content of Al_2O_3 in the coating decreases, and the microhardness decreases. As a result, the plating temperature should be controlled at about 55°C.

3.3. Effect of Current Density on Microhardness of Composite Coating. Figure 4 shows the relationship between the current density and the hardness of the composite coating when the plating temperature is 55°C and the pH value is 4.5. As the current density increases, the microhardness of the coating gradually increases. When the current density is 1 A/dm^2, the microhardness reaches the maximum, and the current density increases further, the hardness of the coating decreases inversely. This is because, with the increase of current density, the current efficiency increases and the content of Al_2O_3 sol in the sedimentary layer are increased per unit time. Too high current density will cause the rate of Al_2O_3 sol embedding into the composite coating to be slower than the deposition rate of matrix metal, thus, reducing the content of Al_2O_3 in the composite coating and decreasing the microhardness of the composite coating [15]. Therefore, the appropriate current density should be 1 A/dm^2.

3.4. Effect of Al_2O_3 Sol on Microhardness of Composite Coating. Figure 5 shows the influence of Al_2O_3 sol dosage on the composite coating when the current density is 1 A/dm^2, pH value is 4.5, and the bath temperature is 55°C. It is clear that by adding more nanosol to the bath, the hardness increases to a maximum value of 569 HV for Ni–P–(sol)Al_2O_3 and then decreases. On one hand, Al_2O_3 nanoparticles can act as a barrier against plastic deformation and increase microhardness of the coating by preventing the movement of dislocations [32, 33]. On the other hand, nanoparticles improved the grain refinement of the matrix and hence favor the higher microhardness of nanocomposite coating (Figure 6) [11]. When the amount of sol is 80 ml/L, the microhardness is 569 HV; when the amount of sol in the plating solution is less than 80 ml/L, as the amount of sol increases, the amount of Al_2O_3 particles deposited on the surface of the substrate increases, and the increased chance of being trapped into the coating, so that the coating hardness increases [17]; When the content of Al_2O_3 sol in the plating solution is too much, some Al_2O_3 particles may sink to the bottom without participating in the growth of coating, resulting in uneven deposition of Al_2O_3 particles in the composite coating (Table 3). In addition, high alumina concentration reduces the reduction efficiency of matrix metal, thus, reducing the microhardness of composite coating, inconsistent with the literature report. [34]. It can find that when the dosage of Al_2O_3 sol is 80 ml/L, the coating microhardness is better.

3.5. Microstructure and Composition Analysis of Coating. According to the above results, the current density 1 A/dm^2, pH value 4.5, bath temperature 55°C, and sol dosage 80 ml/L were selected in this study to prepare Ni–P–(sol)Al_2O_3 composite coating. Figures 7(a) and 7(b) are the micromorphologies of Ni–P alloy coating and Ni–P–(sol)Al_2O_3 nanocomposite coating, respectively. Figure 8 demonstrates that the Ni–P–(sol)Al_2O_3 alloy coating deposited with these conditions has good quality and a uniform and smooth surface texture without porosity. Figure 9 is the

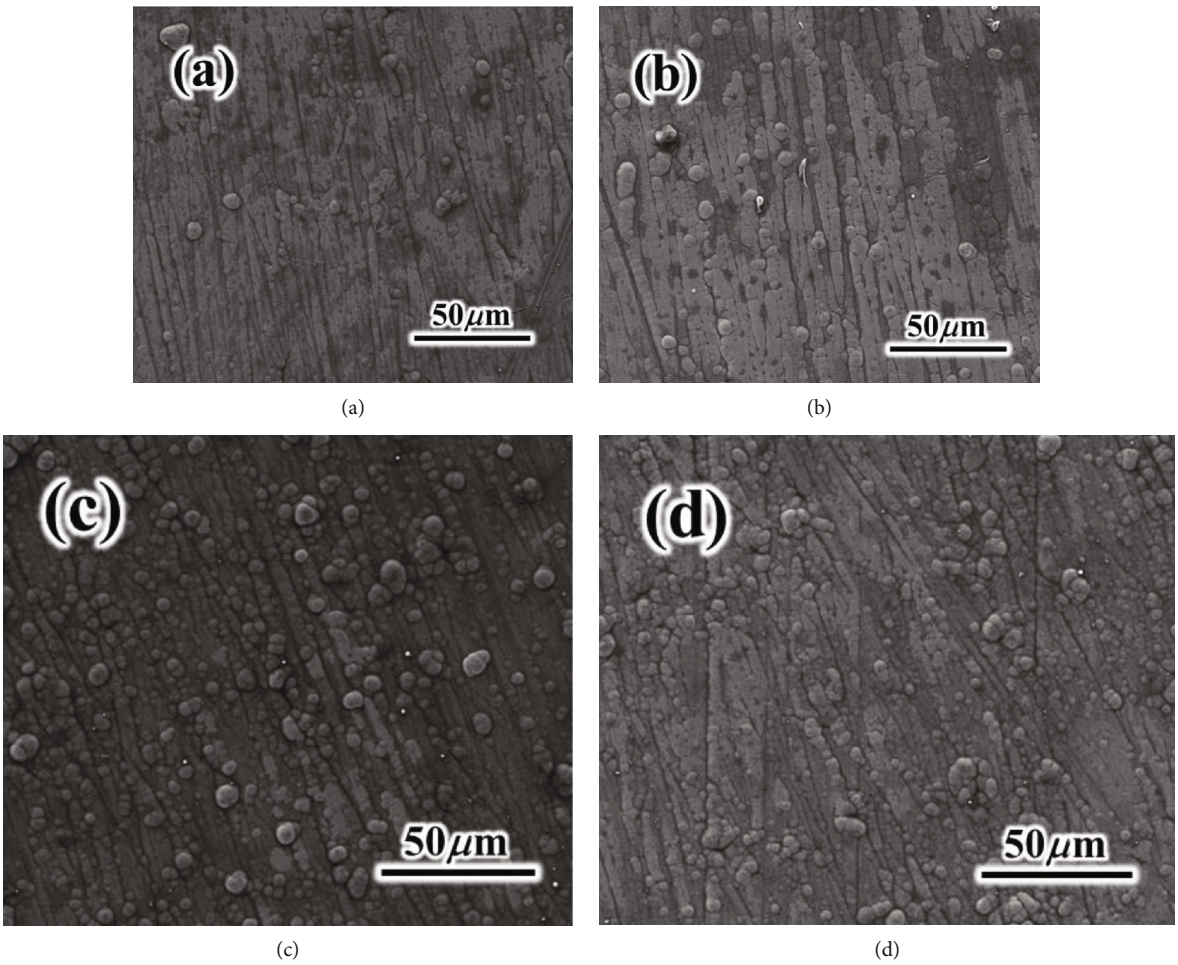

Figure 6: Surface morphology of coatings prepared under different current Al_2O_3 sol dosage (a) 40 mL/L, (b) 60 mL/L, (c) 80 mL/L, and (d) 100 mL/L.

Table 3: Aluminum content of coatings prepared under different Al_2O_3 sol dosage.

Sol dosage (mL/L)	40	60	80	100
Atomic percentage of Al element	0.63	1.29	3.87	1.09

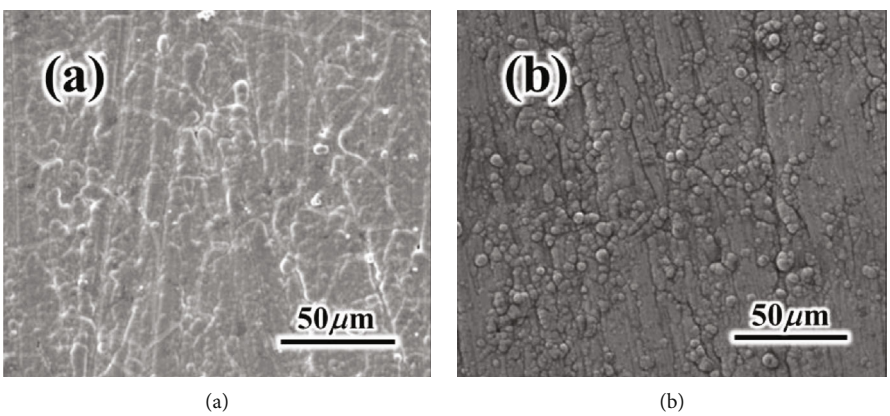

Figure 7: SEM images of the top surface of the coating. (a) Ni–P coating, (b) Ni–P–(sol)Al_2O_3 coating.

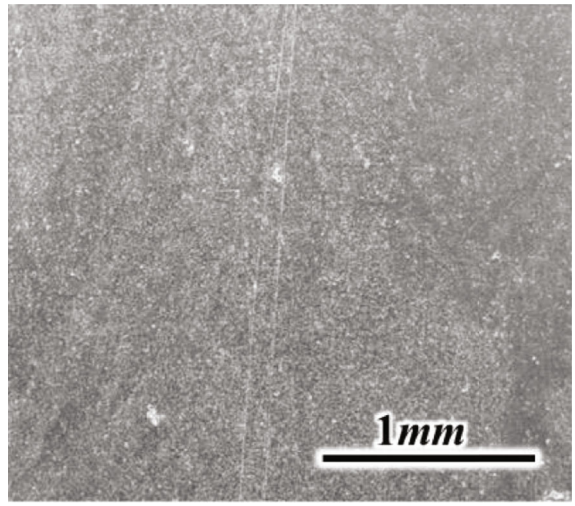

Figure 8: SEM image of the surface morphology of the optimized Ni–P–(sol)Al_2O_3 alloy coating with a deposition temperature of 55°C, pH of 4.5, and current density of 1 A/dm^2.

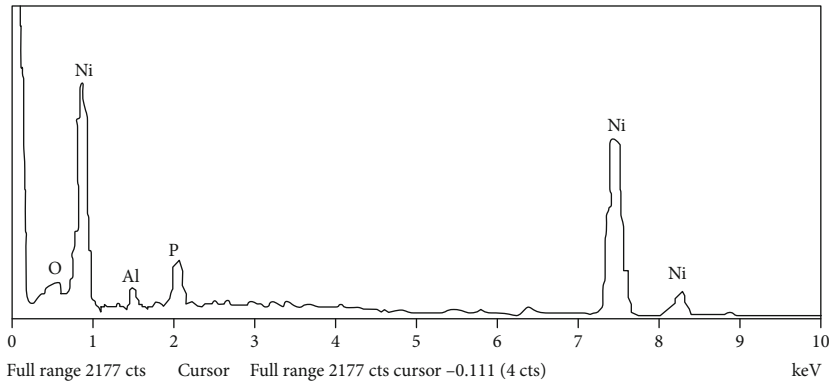

Figure 9: EDS spectrum of the Ni–P–(sol)Al_2O_3 coating with a deposition temperature of 55°C, a pH of 4.5, and a current density of 1 A/dm^2.

EDS spectrum of sol composite coating in Figure 8. It is found that the composite coating contains 3.87% Al, 12.39% P, and 83.74% Ni, which proves the fact that nanoalumina particles in sol enter into the composite coating. As can be seen from Figure 7, pure Ni–P alloy coating has uneven grain size, slight microporous defects, coarse grain size, and uneven surface. The reason may be that in the early electroplating stage, the nickel ion concentration is high and the deposition rate on the substrate surface is fast. The nucleated crystals grow rapidly, and the older crystals prevent the later nucleated crystals from growing. The above results in uneven distribution of crystal size and more surface defects [15]. After the addition of Al_2O_3 sol, the grains are refined, the size is uniform, and the deposition is relatively dense. Because the addition of Al_2O_3 sol increases the cathode polarization in the composite electrodeposition process, leading to the reduction of the nuclear potential of the crystal, which facilitates the formation of a new crystal nucleus of Ni^{2+}. Solutes such as dispersants are contained in the sol, which can inhibit the agglomeration and growth of metal grains. In addition, the incorporation of nanoalumina changes the crystal growth orientation and morphology of the substrate surface significantly. The use of nanoalumina particles as the center of nuclear formation has an inhibitory effect on Ni crystal growth [35]. The particle distribution changes gradually from a scattered distribution to a uniform distribution, and the degree of particle dispersion decreases from large to small, which makes the coating more compact.

3.6. Corrosion Resistance of Nanocomposite Sol Coating. Tafel polarization diagrams for the Electroplate Ni–P and Ni–P–(sol)Al_2O_3 coatings in the as-plated conditions in the 3.5% NaCl solution are shown in Figure 10. Corrosion parameters such as corrosion potential (Ecorr) and the corrosion current density (Icorr) after calculation based on diagrams are presented in Table 4. The obtained data demonstrate that the addition of alumina nanoparticles has resulted in the tendency of the corrosion potential of the Ni–P–(sol)Al_2O_3 composite coating toward more diminished. Also, corrosion current density in the composite coating is lower than that of the Ni–P. This is because Al_2O_3 particles are uniformly distributed in the coating, and the coating is relatively compact, reducing the intergranular corrosion in the coating [17, 36]. Owing to the low conductivity

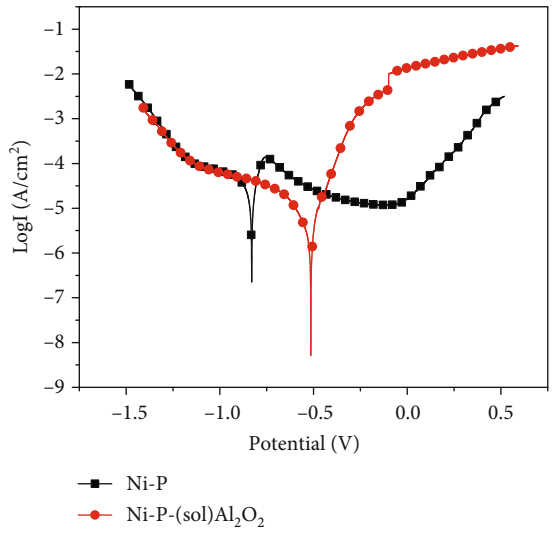

Figure 10: Polarization curves of Ni–P–(sol)Al_2O_3 nanocomposite coating and Ni–P coating in 3.5% NaCl.

Table 4: Important polarization curve parameters.

Coating types	Corrosion potential /V	Corrosion current density (A·cm^{-2})
Ni–P	−0.830	5.67×10^{-4}
Ni–P–(sol)Al_2O_3	−0.514	4.18×10^{-4}

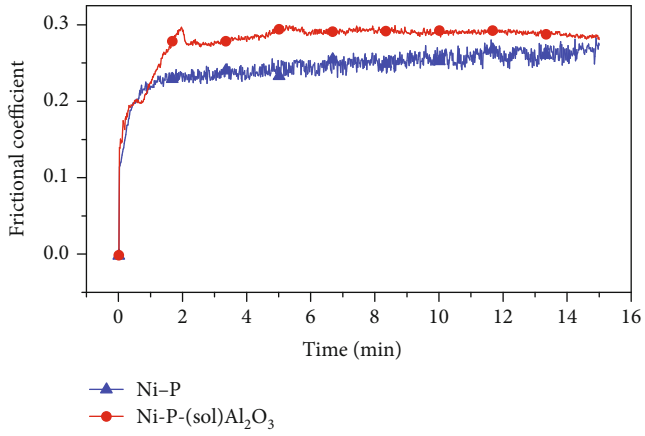

Figure 11: The variation of friction coefficients of two different coatings with time.

of Al_2O_3, the corrosion resistance of Ni–P–(sol)Al_2O_3 composite coating increases.

3.7. Wear Resistance of Composite Sol Coating. Figure 11 displays the variation of coefficient of friction of Ni–P, Ni–P–(sol)Al_2O_3 nanocomposite coatings recorded during the wear test. Wear is a constant and undesirable gradual decrease of the material at the surface during contacting with other materials. The wear mechanisms of the Ni–P coatings are mainly abrasive and adhesive [37]. The coefficient of friction is initiated with the lower values in all the samples and reached maximum value within about two minutes of a sliding test. The friction coefficient of each sample increases rapidly at the initial stage of friction coefficient measurement until reaching an approximately stationary state at greater distance. The premature variation of coefficient of friction in a dry wear process is often referred to as "running" or "break-in" and can be attributed to the formation and rupture of surface oxide films or changes in the geometry of the contact surface [38]. The coefficient of friction varied with the sliding distance in the range 0.1–0.3, values that coincide with reports from the literature [39]. As the friction process proceeds, the surface of the specimen becomes smoother and the friction coefficient tends to be stable due to the plastic deformation of the microprotrusions on the friction contact surface. It can be seen from Table 5 that the friction factor of Ni–P–(sol)Al_2O_3 nanocomposite coating is greater than that of Ni–P coating, while the wear rate of the composite coating is lower than that of Ni–P coating. This is explained by the addition of alumina particles increased the roughness of the coating, partially disappearing the nodular structure but keeping a homogeneous and uniform distribution of the reinforcement [40]. In the process of adding alumina sol to the plating solution, alumina particles enter the coating and microprotuberance occurs inside the coating. These microprotrusions cause the friction coefficient to increase. In addition, Al_2O_3 particles have high hardness and wear resistance, which can support the friction surface load during the friction process, reduce the wear of matrix alloys, and resist plastic deformation. Therefore, the wear resistance of Ni–P–(sol)Al_2O_3 composite coating is higher than that of Ni–P coating.

Table 5: The friction coefficients and wear rate of two types of coatings.

Type of coating	Ni–P	Ni–P–(sol)Al_2O_3
Average friction coefficient	0.2451	0.2799
Wear rate (10^{-6} g·m^{-1})	5.305	1.768

4. Conclusions

Ni–P–(sol)Al_2O_3 composite coating has been produced by the sol-gel and electrodeposition technique. High dispersion nanoalumina particle reinforced composites were prepared. The hardness and corrosion resistance of the coatings prepared by different processing parameters were investigated. The best conditions for electrodeposition of Ni–P–(sol)Al_2O_3 composite coating are pH 4.5, temperature 55°C, current density 1 A/dm^2, and the dosage of Al_2O_3 sol are about 80 ml/L. Ni–P–(sol)Al_2O_3 composite coating has finer and more uniform grains, denser deposition, and higher hardness than pure Ni–P coating. The corrosion current densities of Ni–P coating and Ni–P–(sol)Al_2O_3 coating are 5.57×10^{-4} A/cm^2 and 4.18×10^{-4} A/cm^2, respectively. Corrosion resistance in 3.5%NaCl solution was improved compared with Ni–P

coating. Compared with Ni–P coating, Ni–P–(sol)Al_2O_3 composite coating has better friction and wear properties.

Data Availability

The data used to support the findings of this study are available from the corresponding author upon request.

Conflicts of Interest

The authors declare that they have no conflicts of interest.

Acknowledgments

The authors gratefully acknowledge the supports from the Key Scientific Research Projects of Higher Education of Henan Province of China (Grant no. 19A430014), the Young Key Teachers Projects in Henan Higher Education Institutions (Grant no. 2018GGJS113), the Scientific and Technological Research Projects of Henan Province (Grant no. 192102210215), and the Program for Innovative Research Team (in Science and Technology) in University of Henan Province (Grant no. 20IRTSTHN016).

References

[1] X. H. Zhang, X. X. Li, W. J. Liu, Y. Q. Fan, H. Chen, and T. X. Liang, "Preparation and tribological behavior of electrodeposited Ni–W–GO composite coatings," *Rare Metals*, vol. 38, no. 7, pp. 695–703, 2019.

[2] T. Suzuki, M. Kato, T. Matsuda, and S. Kobayashi, "High temperature hardness of electrodeposited nickel-based carbon nanotube composite coatings," *ECS Transactions*, vol. 50, no. 52, pp. 165–169, 2013.

[3] A. Zarebidaki and S. R. Allahkaram, "Porosity measurement of electroless Ni–P coatings reinforced by CNT or SiC particles," *Surface Engineering*, vol. 28, no. 6, pp. 400–405, 2013.

[4] Y. Li, C. Fu, L. Liu, M. Liang, Y. Liu, and W. Gao, "Influence of temperature and pH value on deposition rate and corrosion resistance of Ni–Zn–P alloy coating," *International Journal of Modern Physics B*, vol. 33, article 1940013, 2019.

[5] A. Zoikis-Karathanasis, E. A. Pavlatou, and N. Spyrellis, "Pulse electrodeposition of Ni–P matrix composite coatings reinforced by SiC particles," *Journal of Alloys and Compounds*, vol. 494, no. 1-2, pp. 396–403, 2010.

[6] L. Yongfeng, Z. Limin, W. Zhankui et al., "Ni-P TiO_2 nanoparticle composite formed by chemical plating: deposition rate and corrosion resistance," *International Journal of Electrochemical Science*, vol. 12, pp. 3385–3397, 2017.

[7] T. R. Tamilarasan, R. Rajendran, G. Rajagopal, and J. Sudagar, "Effect of surfactants on the coating properties and corrosion behaviour of Ni–P–nano-TiO_2 coatings," *Surface & Coatings Technology*, vol. 276, pp. 320–326, 2015.

[8] W. Chen, W. Gao, and Y. He, "Sol-enhanced triple-layered Ni–P–TiO_2 composite coatings," *Journal of Sol-Gel Science and Technology*, vol. 55, no. 2, pp. 187–190, 2010.

[9] S. Mohajeri, A. Dolati, and S. Rezagholibeiki, "Electrodeposition of Ni/WC nano composite in sulfate solution," *Materials Chemistry and Physics*, vol. 129, no. 3, pp. 746–750, 2011.

[10] S.-Y. Tian, J. Ma, R.-J. Ying, and S.-L. Mu, "Corrosion behaviour of Ni–P–SiO_2 electroless composite coating," in *Proceedings of the 2016 7th International Conference on Mechatronics, Control and Materials (ICMCM 2016)*, vol. 104, pp. 447–451, Changsha, Hunan, China, 2016.

[11] S. Sadreddini, A. Afshar, and M. A. Jazani, "Tribological properties of Ni–P–SiO_2 nanocomposite coating on aluminum," *Colloid Journal*, vol. 77, no. 5, pp. 628–634, 2015.

[12] S. Ankita and A. K. Singh, "Corrosion and wear resistance study of Ni-P and Ni-P-PTFE nanocomposite coatings," *Open Engineering*, vol. 1, no. 3, pp. 234–243, 2011.

[13] I. R. Mafi and C. Dehghanian, "Comparison of the coating properties and corrosion rates in electroless Ni–P/PTFE composites prepared by different types of surfactants," *Applied Surface Science*, vol. 257, no. 20, pp. 8653–8658, 2011.

[14] F. Tabatabaei, S. Vardak, S. Alirezaei, and K. Raeissi, "The tribocorrosion behavior of Ni–P and Ni–P–ZrO_2 coatings," *Metallic Materials*, vol. 56, no. 6, pp. 379–387, 2018.

[15] D. Vojtěch, "Properties of Hard Ni–P–Al2O3and Ni–P–SiC Coatings on Al-Based Casting Alloys," *Materials and Manufacturing Processes*, vol. 24, no. 7-8, pp. 754–757, 2009.

[16] S. Alirezaei, S. M. M. Vaghefi, M. Ürgen, A. Saatchi, and K. Kazmanli, "Evaluation of structure and mechanical properties of Ni–P–Al2O3nanocomposite coatings," *Journal of Composite Materials*, vol. 47, no. 26, pp. 3323–3329, 2012.

[17] A. Sharma and A. K. Singh, "Electroless Ni-P and Ni-P-Al_2O_3 nanocomposite coatings and their corrosion and wear resistance," *Journal of Materials Engineering and Performance*, vol. 22, no. 1, pp. 176–183, 2013.

[18] H. H. Sheu, P. C. Huang, L. C. Tsai, and K. H. Hou, "Effects of plating parameters on the Ni–P–Al_2O_3 composite coatings prepared by pulse and direct current plating," *Surface & Coatings Technology*, vol. 235, no. 22, pp. 529–535, 2013.

[19] W. C. Sun, M. F. Tan, J. H. Lu, L. Zhang, and Q. Zhou, "Corrosion and oxidation resistance of electroless Ni-P-Al₂O₃ composite coatings on carbon steel," *Applied Mechanics and Materials*, vol. 34-35, pp. 831–835, 2010.

[20] J. N. Balaraju, Kalavati, and K. S. Rajam, "Influence of particle size on the microstructure, hardness and corrosion resistance of electroless Ni–P–Al_2O_3 composite coatings," *Surface & Coatings Technology*, vol. 200, no. 12-13, pp. 3933–3941, 2006.

[21] W. Chen, W. Gao, and Y. He, "A novel electroless plating of Ni–P–TiO_2 nano-composite coatings," *Surface & Coatings Technology*, vol. 204, no. 15, pp. 2493–2498, 2010.

[22] W. Chen, Y. He, and W. Gao, "Electrodeposition of sol-enhanced nanostructured Ni-TiO_2 composite coatings," *Surface & Coatings Technology*, vol. 204, no. 15, pp. 2487–2492, 2010.

[23] A. Sadeghzadeh-Attar, G. AyubiKia, and M. Ehteshamzadeh, "Improvement in tribological behavior of novel sol-enhanced electroless Ni-P- SiO_2 nanocomposite coatings," *Surface & Coatings Technology*, vol. 307, pp. 837–848, 2016.

[24] A. Rahman and R. Jayaganthan, "Effect of pH values on nanostructured Ni–P films," *Applied Nanoscience*, vol. 5, no. 4, pp. 493–498, 2015.

[25] K. D. R. N. Kalubowila, K. M. D. C. Jayathileka, L. S. R. Kumara et al., "Effect of bath pH on electronic and morphological properties of electrodeposited Cu_2O thin films," *Journal of The Electrochemical Society*, vol. 166, no. 4, pp. D113–D119, 2019.

[26] M. Czagany and P. Baumli, "Effect of pH on the characteristics of electroless Ni–P coatings," *Journal of Mining and Metallurgy, Section B: Metallurgy*, vol. 53, no. 3, pp. 327–332, 2017.

[27] A. M. Rashidi and A. Amadeh, "The effect of saccharin addition and bath temperature on the grain size of nanocrystalline nickel coatings," *Surface & Coatings Technology*, vol. 204, no. 3, pp. 353–358, 2009.

[28] H. Natter and R. Hempelmann, "Nanocrystalline metals prepared by electrodeposition," *Zeitschrift für Physikalische Chemie*, vol. 222, no. 2-3, pp. 319–354, 2008.

[29] D. R. Turner, "The effect of temperature on the cathode potential during nickel plating," *Journal of the Electrochemical Society*, vol. 100, no. 1, pp. 15–21, 1953.

[30] W. H. Li, X. Y. Zhou, Z. Xu, and M. J. Yan, "Effect of bath temperature on nanocrystalline Ni-polytetrafluoroethylene composite coatings prepared by brush electroplating," *Surface Engineering*, vol. 25, no. 5, pp. 353–360, 2013.

[31] H. J. Zhang, C. Li, X. L. Ru, C. D. Zhang, and C. C. Chen, "Effect of temperature on the performances of co-W-P alloy coatings prepared by electroless plating," *Electroplating & Pollution Control (China)*, vol. 37, no. 3, pp. 30–32, 2017.

[32] M. Habibnejad-Korayem, R. Mahmudi, H. M. Ghasemi, and W. J. Poole, "Tribological behavior of pure Mg and AZ31 magnesium alloy strengthened by Al_2O_3 nano-particles," *Wear*, vol. 268, no. 3-4, pp. 405–412, 2010.

[33] N. Ghavidel, S. R. Allahkaram, R. Naderi, M. Barzegar, and H. Bakhshandeh, "Corrosion and wear behavior of an electroless Ni-P/nano-SiC coating on AZ31 Mg alloy obtained through environmentally-friendly conversion coating," *Surface & Coatings Technology*, vol. 382, article 125156, 2020.

[34] R. Hu, Y. Su, Y. Liu et al., "Deposition process and properties of electroless Ni-P-Al_2O_3 composite coatings on magnesium alloy," *Nanoscale Research Letters*, vol. 13, no. 1, p. 198, 2018.

[35] Q. Feng, T. Li, H. Yue, K. Qi, F. Bai, and J. Jin, "Preparation and characterization of nickel nano-Al_2O_3 composite coatings by sediment co-deposition," *Applied Surface Science*, vol. 254, no. 8, pp. 2262–2268, 2008.

[36] R. C. Agarwala, V. Agarwala, and R. Sharma, "Electroless Ni-P Based Nanocoating Technology—A Review," *Synthesis and Reactivity in Inorganic, Metal-Organic, and Nano-Metal Chemistry*, vol. 36, no. 6, pp. 493–515, 2007.

[37] D. T. Gawne and U. Ma, "Wear mechanisms in electroless nickel coatings," *Wear*, vol. 120, no. 2, pp. 125–149, 1987.

[38] P. J. Blau, "Interpretations of the friction and wear break-in behavior of metals in sliding contact," *Wear*, vol. 71, no. 1, pp. 29–43, 1981.

[39] S. Kundu, S. K. Das, and P. Sahoo, "Tribological behaviour of electroless Ni-P deposits under elevated temperature," *Silicon*, vol. 10, no. 2, pp. 329–342, 2018.

[40] C. A. León-Patiño, J. García-Guerra, and E. A. Aguilar-Reyes, "Tribological characterization of heat-treated Ni-P and Ni-P-Al_2O_3 composite coatings by reciprocating sliding tests," *Wear*, vol. 426-427, pp. 330–340, 2019.